RESEARCH ON THE YAW ANGLE CONTROL STRATEGY OF HEXAPOD ROBO WITH TACTILE SENSOR FEEDBACK

Qian Wang,* Bo Jin*,**, Ce Zhang,*** and Shidong Zhang*

Abstract

This paper presents a straightforward yet effective yaw angle feedback control strategy for a hexapod walking robot. The robot's motion is corrected using the yaw angle provided by an IMU module. Kinematic models were analysed for both straight and turning gaits, and a PD controller was implemented for closed-loop control. Additionally, the tactile sensors on the foot tips were used to detect ground contact of the swing legs, and the foot trajectories were adjusted in real-time to minimise attitude deviations. The experiment results confirmed the effectiveness of the proposed strategies.

Key Words

Hexapod robot, yaw angle control, ground contact feedback

1. Introduction

Compared to wheeled robots, multi-legged robots demonstrate superior performances when navigating rough terrains or overcoming obstacles. Among legged robots, hexapod robots exhibit greater walking stability and more gaits than bipedal or quadrupedal robots. Furthermore, hexapod robots can walk with some leg failures [1]. In recent years, various hexapod walking robots have been developed, such as the LAURON V [2], the DLR Crawler [3], the Little Crabster200 [4], and so on.

To enhance the performance and practicality of hexapod robots, numerous studies have been conducted to design control strategies based on the basic robotmotion control scheme and sensing feedback information [5]–[7]. Previous studies have proposed various feedback control strategies for hexapod robots to meet different requirements [8]–[10].

The posture of hexapod robots can fluctuate during walking due to mechanical errors, foot slippage, and other factors [11]. To enhance the walking performance of the robot, it is crucial to develop control strategies that based on the feedback of the attitude angle. Tikam *et al.* introduced a virtual model control (VMC) method, incorporating a novel position-based foot force controller that facilitates direct force control during the leg's stance phase and active compliance control during the swing phase [12]. Chen *et al.* proposed a walking control strategy, based on multi-sensor information feedback, which focus on addressing the vertical contact impact and horizontal sliding issues of heavy legged robots [13]. The six-legged walking robot platform, designed by ZJU, features three joints and a semi-round foot on each leg. By employing inverse velocity kinematics, the research team has studied a posture control strategy that improves the robot's walking ability on rough terrain [14].

Walking on uneven terrain is a crucial task for legged robots. In order to do it successfully, each robot's leg should adapt to the different heights of terrain on which it steps. There are many researches of hexapod robots for walking on the uneven terrain [15]–[17]. Some hexapod robots adapt to uneven terrain with some utilising special structures [18]. RHex can overcome the uneven terrain by rotating its arc-shaped leg sequentially, but this method could mess up the environment [19]. Deng *et al.* established a gait library with different kinds of gaits which enables hexapod robots to walk through dynamic environments [20]. Some researches adapt central pattern generator (CPG) to realise locomotion on the uneven terrain [21]–[23]. While the CPG is a popular method for achieving uneven terrain locomotion, it is not ideal for precise robot motion. Compliance control methods have also been employed to reduce impact and ensure stable walking on different kinds of ground [24], [25].

In our previous work [26], we have studied the straight gait planning and gait transformation between multiple gaits. We proposed a yaw angle control algorithm

* State Key Laboratory of Fluid Power and Mechatronic Systems, Zhejiang University, Hangzhou 310027, China; e-mail: {bjin, qian_wang, 21825076}@zju.edu.cn
** Ningbo Research Institute, Zhejiang University, Ningbo 315100, China
*** Ningbo Hoyea Machinery Manufacture Co., Ltd., Ningbo 315100, China; e-mail: ce.zhang@hoyea.com
Corresponding author: Bo Jin

Recommended by Xin Xu
(DOI: 10.2316/J.2024.206-0857)

(a)

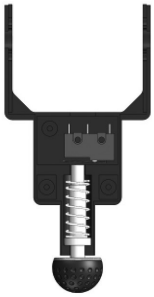

(b)

Figure 1. The hexapod walking robot HexWalker II: (a) the hexapod robot; and (b) the structure of the robot's foot.

for straight gait based on kinematics analysis and PD controller. In this paper, we aim to further investigate the yaw angle control method by analysing the kinematic analysis for both straight and turning gaits. We will also utilise the tactile sensors on the foot tips to detect ground contact and adjust the foot trajectories of swing legs.

The remainder of this paper is organised as follows: Section 2 presents a brief introduction of the hexapod robot HexWalker II, including its kinematic model analysis and basic control method. Section 3 discusses the yaw angle control strategy and ground contact strategy. Section 4 demonstrates the experimental results. Finally, Section 5 concludes the paper.

2. Basic Control Method of the Robot

2.1 Overview of the Hexapod Robot

The HexWalker II is a small electric hexapod robot weighing approximately 3 kg and has dimensions of roughly 268 mm × 166 mm × 275 mm, as shown in Fig. 1. The robot has a total of 18 degrees of freedom (DOFs), with each leg consisting of three DOFs, including the root, hip, and knee joints from top to bottom, driven by FEETECH servo motors. These servo motors can be controlled through serial ports and can provide feedback on their current positions.

Each leg has a tactile sensor located on the foot-tip that detects contact with the ground. The tactile sensor is made up with a micro switch and a spring, providing a simple yet effective method of detecting the contact between the robot's foot and the ground.

The main control board of the HexWalker II is Raspberry 3B+, which executes the control algorithm and transmits joint angles to the lower board *via* SPI bus. An IMU module is installed on the robot to obtain the actual attitude information. The STM32-based lower board controls all servo motors, communicates with an IMU module *via* serial ports, and reads the signals of the tactile sensors.

The main control algorithm of the robot is shown in Fig. 2. According to the expected motion, the foot trajectory planning and gait planning are designed to determine the desired foot positions. The foot trajectory planning and gait planning can be adjusted according to sensor feedback. The desired angle of each joint is calculated by inverse kinematics, and the servo motors are driven to control the robot's motion accordingly.

2.2 Kinematic Modelling

The coordinate frames of the robot are shown in Fig. 3. The global coordinate frame is denoted as $\{W\}$. Frame $\{B\}$ represents the body frame, situated at the center of the robot's body. Take leg 1 as an example, the frames of the legs are shown in Fig. 3(b). These frames are established based on the Denavit–Hartenberg (D–H) rules, with frame $\{O_{i,L}\}(i = 1, \dots 6)$ as the base frame of each leg, and frames $\{O_{i,0}\}$, $\{O_{i,1}\}$, $\{O_{i,2}\}$, $\{O_{i,3}\}(i = 1, \dots 6)$ as joint frames of each leg. During the robot's locomotion, the desired position of each leg's foot-tip is described by its leg trajectory with reference to the leg base frame $\{O_{i,L}\}$, and the joint angles are computed using the position *via* inverse kinematics.

2.2.1 Forward Kinematics

Take leg 1 as an example, the D–H parameters of leg 1 are listed in Table 1. The transformation matrix between the leg base frame $\{O_{i,L}\}$ and the root joint frame $\{O_{i,0}\}$ can be expressed as:

$$ {}^{L}_{0}T_i = \begin{bmatrix} 0 & 0 & 1 & 0 \\ 0 & 1 & 0 & 0 \\ -1 & 0 & 0 & 0 \\ 0 & 0 & 0 & 1 \end{bmatrix} \tag{1} $$

The transformation matrix between two adjacent joint frames $\{O_{i,j}\}, \{O_{i,j-1}\}(j = 1, 2, 3)$ can be expressed as:

$$ {}^{j-1}_{j}T_i = \begin{bmatrix} s\theta_{i,j} & -s\theta_{i,j}c\alpha_{i,j} & s\theta_{i,j}s\alpha_{i,j} & a_i c\theta_{i,j} \\ s\theta_{i,j} & c\theta_{i,j}c\alpha_{i,j} & -c\theta_{i,j}s\alpha_{i,j} & a_i s\theta_{i,j} \\ 0 & s\alpha_{i,j} & c\alpha_{i,j} & d_{i,j} \\ 0 & 0 & 0 & 1 \end{bmatrix} \tag{2} $$

Where $\theta_{i,j}, d_{i,j}, a_{i,j},$ and $\alpha_{i,j}$ are the D–H parameters and $c\theta_{i,j}$ and $s\theta_{i,j}$ denote cosine and sine of $\theta_{i,j}$, respectively.

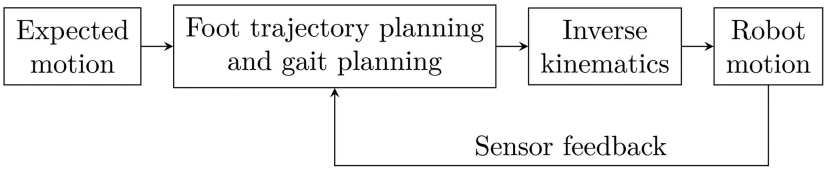

Figure 2. Main control algorithm of the robot.

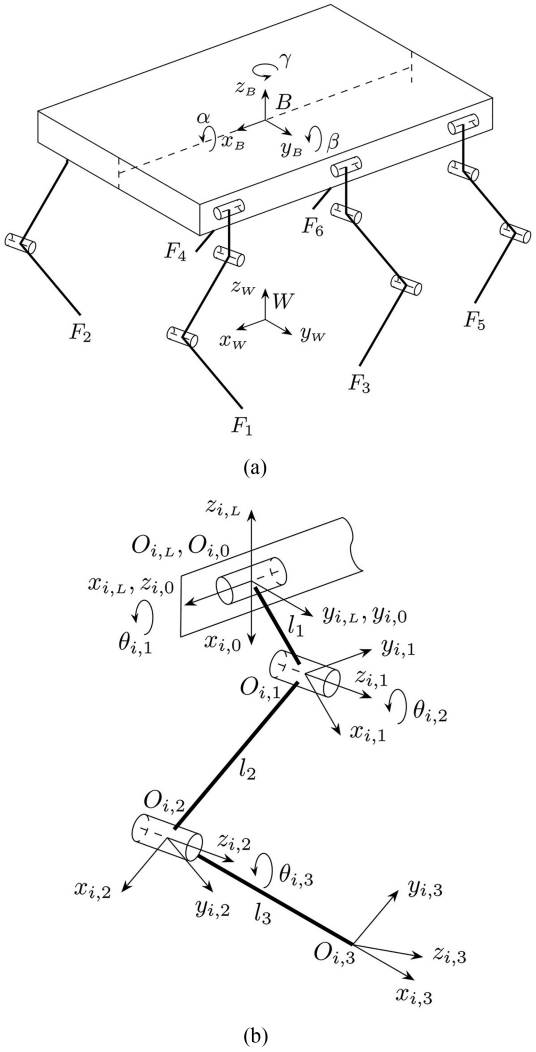

Figure 3. Frames of the hexapod robot: (a) frames of the robot; and (b) frames of the leg.

The position of the foot-tip P_i, with respect to the base frame of each leg, can be described as:

$$\begin{bmatrix} {}^{L}P_{F_i} \\ 1 \end{bmatrix} = \begin{bmatrix} P_{i,x} \\ P_{i,y} \\ P_{i,z} \\ 1 \end{bmatrix} = {}^{L}_{0}T_i\ {}^{0}_{1}T_i\ {}^{1}_{2}T_i\ {}^{2}_{3}T_i$$
$$= \begin{bmatrix} -s\left(\theta_{i,2}+\theta_{i,3}\right)l_3 - s\theta_{i,2}l_2 \\ s\theta_{i,1}c\left(\theta_{i,2}+\theta_{i,3}\right) + s\theta_{i,1}c\theta_{i,2}l_2 + s\theta_{i,1}l_1 \\ -c\theta_{i,1}c\left(\theta_{i,2}+\theta_{i,3}\right) - c\theta_{i,1}c\theta_{i,2}l_2 - c\theta_{i,1}l_1 \\ 1 \end{bmatrix} \quad (3)$$

Table 1
Values of the Denavit–Hartenberg Parameters

Link j	$\theta_{i,j}(^\circ)$	$d_{i,j}$(mm)	$a_{i,j}$(mm)	$\alpha_{i,j}(^\circ)$
1	$\theta_{i,1}$	0	l_1	-90
2	$\theta_{i,2}$	0	l_2	0
3	$\theta_{i,3}$	0	l_3	0

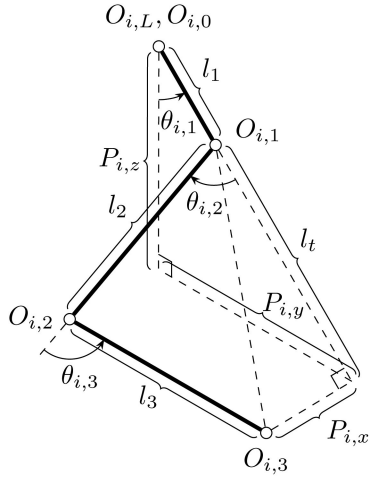

Figure 4. Schematic of inverse kinematics.

2.2.2 Inverse Kinematics

The inverse kinematics equations can be derived by the geometric approach based on the robot's joint configuration. As an example, for leg 1 shown in Fig. 4, the inverse kinematic equations can be given as:

$$\begin{aligned} \theta_{i,1} &= -\arctan\frac{P_{i,y}}{P_{i,z}} \\ \theta_{i,2} &= -\arccos\frac{l_2^2-l_3^2+l_t^2+P_{i,x}^2}{2l_2\sqrt{P_{i,x}^2+l_t^2}} - \arctan\frac{P_{i,x}}{l_t} \\ \theta_{i,3} &= \arccos\frac{-l_2^2-l_3^2+l_t^2+P_{i,x}^2}{2l_2l_3} \end{aligned} \quad (4)$$

Where $l_t = \sqrt{P_{i,y}^2 + P_{i,z}^2} - l_1$

2.3 Foot Trajectory Planning

The walking motion of the robot's legs is comprised of the swing phase and stance phase. Foot trajectory planning involves determining the complete trajectory of the foot of leg i as it moves relative to the base frame of the leg $\{O_{i,L}\}$, while taking into account gait parameters and sensor feedback during walking. For better adaptation to the uneven terrain, the foot trajectory during the swing phase is divided into three parts, namely, the swing-up

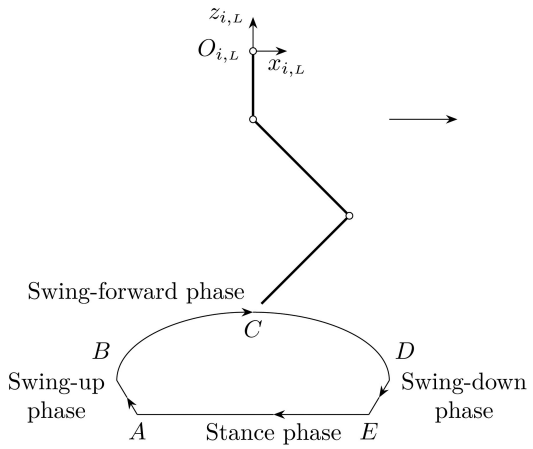

Figure 5. Schematic of foot trajectory planning.

phase, the swing-forward phase, and the swing-down phase, as illustrated in Fig. 5.

For example, in the case of the straight gait while the foot end position in the y direction is always 0, Fig. 5 displays the foot trajectory relative to frame $\{O_{i,L}\}$ in the $x - z$ plane.

During the swing-up phase ($A-B$) and the swing-down phase ($D - E$), straight lines are used to plan the foot trajectories to avoid collisions with obstacles and accommodate for possible early landing or late landing on uneven terrain. The speed in the x direction is opposite to the forward speed of the robot so that the foot trajectory in the world frame is straight up and down.

During the swing-forward phase ($B - C - D$) and the stance phase ($E - A$), the foot trajectories are planned as sixth-order polynomial curves. These curves are fitted separately in the x, y, and z directions, based on the constraints of foot position, velocity, and acceleration at the initial and end time. This approach enables a smooth connection between the trajectories in the four phases and eliminates sudden changes in speed.

2.4 Gait Planning

The robot's walking gait determines the time sequences of the swing and support phases of one leg. The periodic gaits are used for gait planning, including the tripod gait, quadrangular gait, and pentagonal gait. The robot can walk straight or turn around with a specified gait, and it has the ability to switch between different gaits either while walking straight or turning. Additional details are available in [26].

3. The Details of the Control Strategy

In Section 2, the robot exhibits some rudimentary open-loop motion capabilities. Nevertheless, variations in attitude may arise while traversing flat terrain due to mechanical inaccuracies and jolts when lifting or landing its legs. Hence, incorporating sensor feedback becomes essential to a certain extent in achieving closed-loop control for enhancing walking performance.

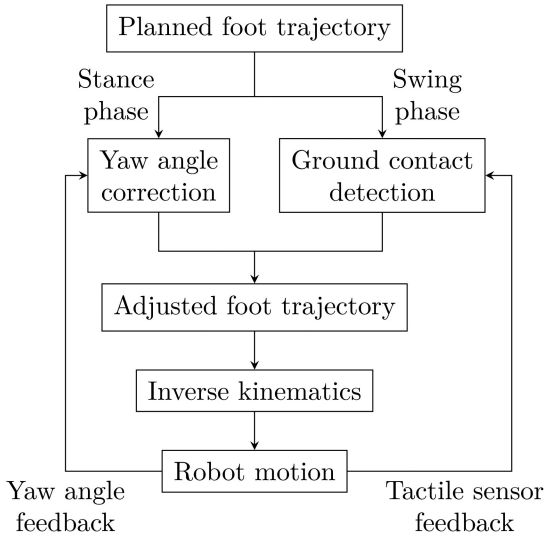

Figure 6. Schematic of feedback control strategy.

In our previous work, we implemented a yaw angle correction algorithm based on kinematic analysis for straight gait, which effectively minimised the yaw angle deviation. In this paper, we have extended the yaw angle correction algorithm to encompass both straight and turning gaits. Furthermore, we have integrated a straightforward ground contact feedback approach to further diminish postural instability. As illustrated in Fig. 6, the planned foot trajectory will be corrected through yaw angle feedback and tactile sensor feedback, respectively, in the stance and swing phases.

3.1 Yaw Angle Feedback

During walking, the robot may experience posture deviations. Compared to pitch and roll angles, the yaw angle has less influence on the stability of robot walking, but it's critical for accurate robot positioning. Failure to correct the yaw angle error promptly can lead to significant deviation from the intended trajectory. Therefore, the yaw angle correction algorithm is designed to reduce the robot motion error by leveraging actual yaw angle information from an IMU module on the robot.

The algorithm aims to adjust the foot positions of the legs with respect to the body coordinate system $\{B\}$ during the stance phase. This adjustment will enable the robot to move closer to the intended direction, thus correcting the yaw angle in time. A kinematic model is necessary to determine the foot positions after adjustment while considering the walking direction adjustment. Taking the tripod gait as an example, the following sections provide a detailed description of straight gait and turning gait, respectively.

Figure 7(a) depicts the kinematic model for yaw angle correction during straight gait. Suppose there is a deviation $\Delta\gamma$ between the actual direction and the desired direction, and the robot needs to move forward by a distance of Δs in the next moment, which is determined by the originally planned foot trajectory. To reduce the yaw angle error, the robot is desired to rotate around the body frame $\{B\}$

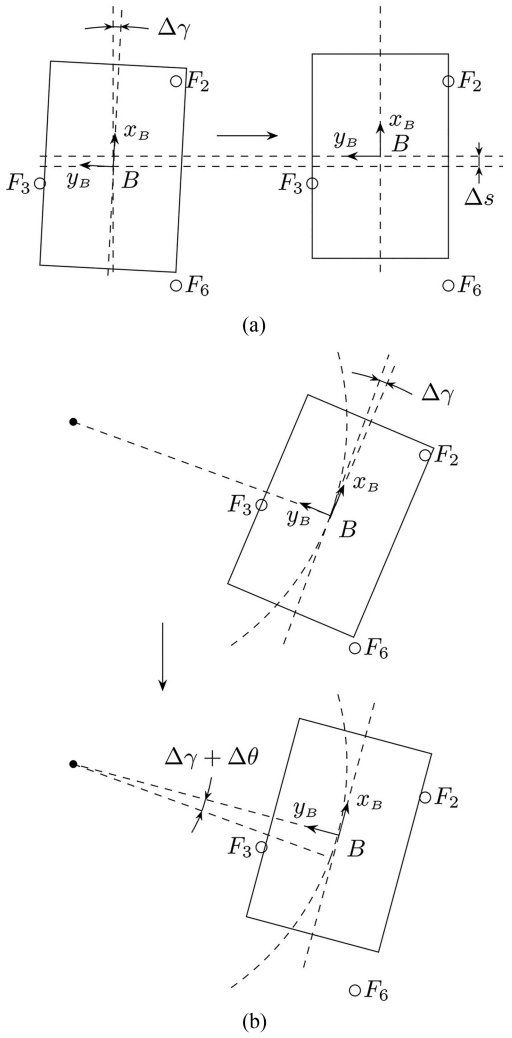

Figure 7. Schematic of yaw angle correction: (a) yaw angle correction in straight gait; and (b) yaw angle correction in turning gait.

to align with the ideal direction, while maintaining its originally forward motion. In the subsequent moment, it's necessary to recalculate the foot position of the supporting legs relative to the body frame $\{B\}$.

Assuming that the foot position of a supporting leg i relative to the body frame $\{B\}$ is $\begin{bmatrix} {}^{B}P_{i,x} & {}^{B}P_{i,y} & {}^{B}P_{i,z} & 1 \end{bmatrix}^T$ at the current moment and $\begin{bmatrix} {}^{B}P'_{i,x} & {}^{B}P'_{i,y} & {}^{B}P'_{i,z} & 1 \end{bmatrix}^T$ in the next moment. We can obtain their relationship as follows:

$$\begin{bmatrix} {}^{B}P_{i,x} \\ {}^{B}P_{i,y} \\ {}^{B}P_{i,z} \\ 1 \end{bmatrix} = R_z(\Delta\gamma) \begin{bmatrix} 1 & 0 & 0 & \Delta\mathrm{s} \\ 0 & 1 & 0 & 0 \\ 0 & 0 & 1 & 0 \\ 0 & 0 & 0 & 1 \end{bmatrix} \begin{bmatrix} {}^{B}P'_{i,x} \\ {}^{B}P'_{i,y} \\ {}^{B}P'_{i,z} \\ 1 \end{bmatrix} \tag{5}$$

Where $R_z(\Delta\gamma)$ denotes the rotation matrix around the z-axis.

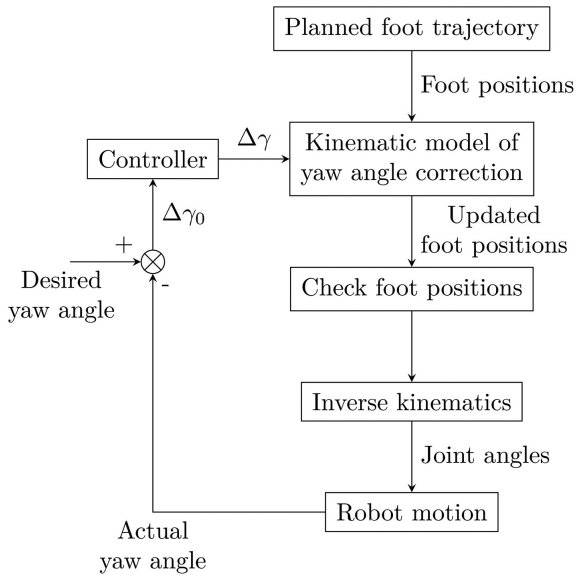

Figure 8. Schematic of yaw angle correction algorithm.

$$R_z(\Delta\gamma) = \begin{bmatrix} \cos\Delta\gamma & -\sin\Delta\gamma & 0 & 0 \\ \sin\Delta\gamma & \cos\Delta\gamma & 0 & 0 \\ 0 & 0 & 1 & 0 \\ 0 & 0 & 0 & 1 \end{bmatrix}$$

Then, we have:

$$\begin{bmatrix} {}^{B}P'_{i,x} \\ {}^{B}P'_{i,y} \\ {}^{B}P'_{i,z} \\ 1 \end{bmatrix} = \begin{bmatrix} {}^{B}P_{i,x}\cos\Delta\gamma + {}^{B}P_{i,y}\sin\Delta\gamma - \Delta\mathrm{s} \\ -{}^{B}P_{i,x}\sin\Delta\gamma + {}^{B}P_{i,y}\cos\Delta\gamma \\ {}^{B}P_{i,z} \\ 1 \end{bmatrix} \tag{6}$$

Figure 7(b) illustrates the kinematic model for yaw angle correction during turning gait. Suppose the robot is turning counterclockwise and is not in an ideal attitude at a certain moment. Similar to the straight gait, the robot needs to rotate to align with an ideal planned yaw angle around the center of the body by an angle $\Delta\gamma$. According to the original gait planning scheme, the robot is planned to rotate around the center of the circle by an angle $\Delta\theta$. To reduce the yaw angle error promptly, the robot needs to rotate around by an angle $\Delta\gamma + \Delta\theta$. Then the desired foot positions in the next moment are determined.

Similar to the straight gait, for a supporting leg i, let the foot position relative to the body frame $\{B\}$ at the current moment and the next moment be $\begin{bmatrix} {}^{B}P_{i,x} & {}^{B}P_{i,y} & {}^{B}P_{i,z} & 1 \end{bmatrix}^T$ and $\begin{bmatrix} {}^{B}P'_{i,x} & {}^{B}P'_{i,y} & {}^{B}P'_{i,z} & 1 \end{bmatrix}^T$, respectively. Then, we have:

$$\begin{bmatrix} {}^{B}P_{i,x} \\ {}^{B}P_{i,y} \\ {}^{B}P_{i,z} \\ 1 \end{bmatrix} = R_z(\Delta\gamma + \Delta\theta) \begin{bmatrix} {}^{B}P'_{i,x} \\ {}^{B}P'_{i,y} \\ {}^{B}P'_{i,z} \\ 1 \end{bmatrix} \tag{7}$$

Where $R_z(\Delta\gamma + \Delta\theta)$ is the rotation matrix around the z-axis.

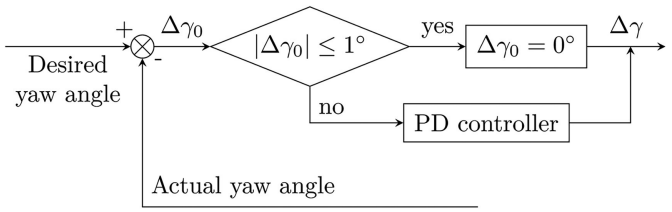

Figure 9. Controller design of yaw angle correction algorithm.

$$R_z\left(\Delta\gamma+\Delta\theta\right)=\begin{bmatrix}\cos\left(\Delta\gamma+\Delta\theta\right) & -\sin\left(\Delta\gamma+\Delta\theta\right) & 0 & 0\\ \sin\left(\Delta\gamma+\Delta\theta\right) & \cos\left(\Delta\gamma+\Delta\theta\right) & 0 & 0\\ 0 & 0 & 1 & 0\\ 0 & 0 & 0 & 1\end{bmatrix}$$

Then, we have:

$$\begin{bmatrix}{}^{B}P'_{i,x}\\ {}^{B}P'_{i,y}\\ {}^{B}P'_{i,z}\\ 1\end{bmatrix}=\begin{bmatrix}{}^{B}P_{i,x}\cos\left(\Delta\gamma+\Delta\theta\right)+{}^{B}P_{i,y}\sin\left(\Delta\gamma+\Delta\theta\right)\\ -{}^{B}P_{i,x}\sin\left(\Delta\gamma+\Delta\theta\right)+{}^{B}P_{i,y}\cos\left(\Delta\gamma+\Delta\theta\right)\\ {}^{B}P_{i,z}\\ 1\end{bmatrix} \quad (8)$$

Based on the kinematic analysis above, the yaw angle correction algorithm can be designed, as illustrated in Fig. 8. For the robot's straight gait, the desired yaw angle is always 0°, while for the turning gait, the desired yaw angle is determined by the gait planning. The robot's actual yaw angle can be acquired from an IMU module. The difference between the actual yaw angle and desired yaw angle $\Delta\gamma_0$ serves as the input of the controller, and the output of the controller $\Delta\gamma$ is the yaw angle bias that is adjusted in the next moment. Before performing the inverse kinematics, the updated foot positions need to be verified to ensure they are within the reachable space, which is determined by the equation $\sqrt{{}^{B}P_{i,x}^{2}+{}^{B}P_{i,y}^{2}+{}^{B}P_{i,z}^{2}} \leq l_1+l_2+l_3$. Foot positions that are outside the reachable space are not updated, instead, the foot positions from the previous moment are maintained. Finally, according to the updated foot positions, the corresponding joint angles of the legs can be obtained using inverse kinematics, and then the servos will be driven to the desired angles to realise the specified motion.

The controller primarily employs a PD controller, as shown in Fig. 9. A threshold value is set for $\Delta\gamma_0$, which is 0° in this case. The walking direction is adjusted only when the difference between the actual and desired yaw angles exceeds the threshold value. The PD controller is utilised to handle the yaw angle deviation, which can mitigate the control error, enhance the system's response speed, and ensure robustness. The PD controller is implemented as follows:

$$\begin{aligned}\Delta\gamma = {} & K_P\left[e\left(k\right)-e\left(k-1\right)\right]\\ & +K_D\left[e\left(k\right)-2e\left(k-1\right)+e\left(k-2\right)\right]\end{aligned} \quad (9)$$

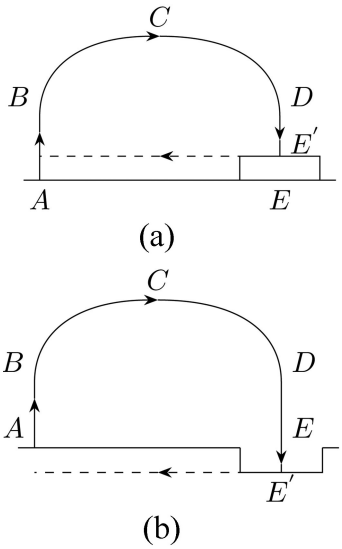

Figure 10. Adjustment of the foot trajectory: (a) early foot landing; and (b) late foot landing.

Where K_P and K_D are the proportional coefficient and differential coefficient, respectively. $e(k)$ is an input deviation of the controller in the k-th sampling.

3.2 Tactile Sensor Feedback

As mentioned in Section 2.3, the robot's foot trajectory is planned using a combination of straight lines and sixth-order polynomial curves. During the swing-up and swing-down phases, the foot trajectories follow straight lines along the z-axis relative to the global coordinate system, this simplifies the avoidance of obstacles and facilitates adaptation to different terrains. To ensure a gradual change in the speed and acceleration, the trajectory during the swing-forward phase is made up of a sixth-degree polynomial.

When traversing uneven terrain, the foot may touch down earlier or later due to obstacles, which differs from the fixed gait circle used when walking on flat ground, as illustrated in Fig. 10. With the tactile sensor on the foot, it's easy to detect whether or not the foot is contact to the ground. Once contact with the ground, the foot transitions from the swing-down phase to the stance phase, and the foot trajectory is then replanned based on the new state. The target landing point for the next cycle remains the same height as before to ensure continuous movement. The gait generator coordinates the sequence of legs entering the swing phase, and the reachability of the foot is checked before movement to guarantee stability and continuity of motion.

4. Experiments

The feasibility and effectiveness of the yaw angle control algorithm and ground contact strategy were verified through several experiments. The robot's parameters were set to a body height of $H = 230$ mm, a total gait circle

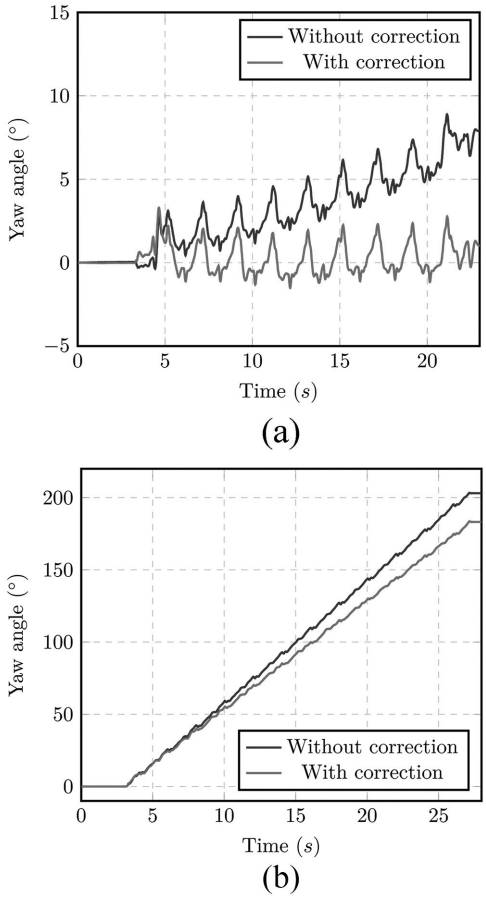

Figure 11. The yaw angle with and without yaw angle correction algorithm: (a) yaw angle correction in straight gait; and (b) yaw angle correction in turning gait.

time $T = 2$ s, and a step length $S = 30$ mm during the experiments.

4.1 Verification of Yaw Angle Correction

The first experiment involved straight walking in the tripod gait with and without the use of the yaw angle correction algorithm. The variation of yaw angle during walking was recorded in Fig. 11(a). The experimental data showed that after several cycles of motion without the yaw angle correction method, the yaw angle approached 9°, possibly due to changes in the body's center of gravity, mechanical error, foot slippage, or other factors. A comparison experiment was conducted using the yaw angle correction algorithm, with the PD controller's parameters set to $K_P = 0.01$ and $K_D = 0.005$, respectively. The variation of the yaw angle was then reduced to within 3° with relatively small deviations after walking.

Similar experiments were conducted for the turning gait, while the robot turned 180° around a circle with a radius of 100 mm. Figure 11(b) shows that without yaw angle correction, the robot ended up with an orientation of around 200°, while the result with yaw angle correction was close to the expected value of 180°.

The efficiency of the ground contact feedback strategy was also verified in two experiments, where the robot

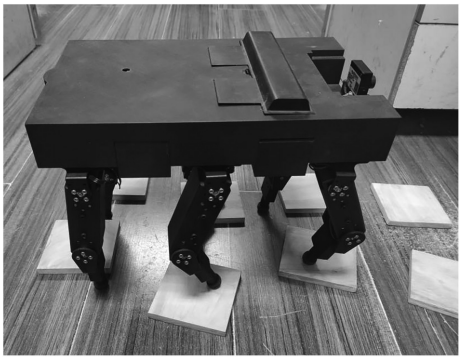

Figure 12. The hexapod robot traversing obstacles.

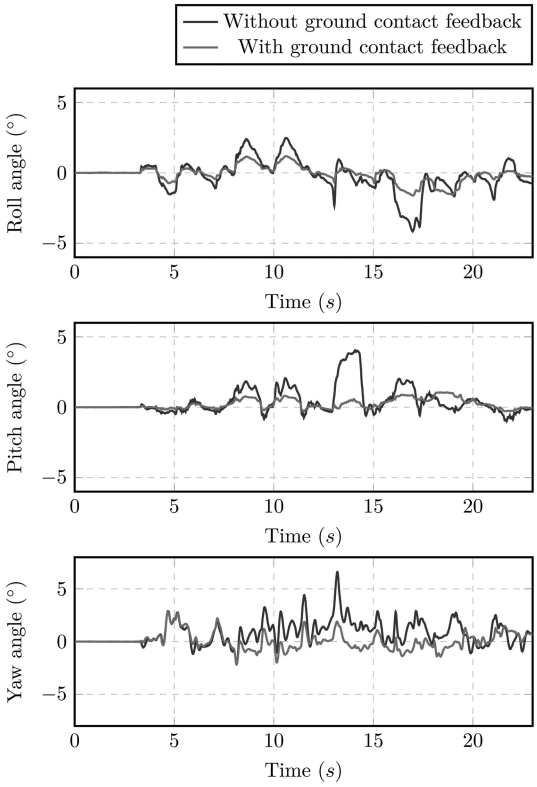

Figure 13. The attitude variations during walking with and without ground contact feedback (with yaw angle correction).

traversed obstacles with a height of about 10 mm, as shown in Fig. 12.

4.2 Verification of Ground Contact Feedback

In the first experiment, with the yaw angle correction enabled, the situations with and without the ground contact feedback strategy are conducted. The attitude variations during walking were recorded in Fig. 13, and Table 2 shows the mean value and standard deviation of the attitude angle. The attitude data demonstrated that the standard deviation of the row angle and the pitch angle was reduced to around 0.5° from 3° using the ground contact feedback strategy, which demonstrated the effectiveness of the method.

Table 2
The Mean μ and Standard Deviation σ of the Orientation Data (With Yaw Angle Correction)

	Roll		Pitch		Yaw	
	$\mu(^\circ)$	$\sigma(^\circ)$	$\mu(^\circ)$	$\sigma(^\circ)$	$\mu(^\circ)$	$\sigma(^\circ)$
Without feedback	−0.212	1.099	0.417	0.972	0.829	1.146
With feedback	−0.093	0.556	0.210	0.339	0.119	0.807

Table 3
The Mean μ and Standard Deviation σ of the Orientation Data (Without Yaw Angle Correction)

	Roll		Pitch		Yaw	
	$\mu(^\circ)$	$\sigma(^\circ)$	$\mu(^\circ)$	$\sigma(^\circ)$	$\mu(^\circ)$	$\sigma(^\circ)$
Without feedback	−0.464	1.217	0.582	1.061	10.798	7.766
With feedback	−0.209	0.448	0.258	0.433	5.078	3.715

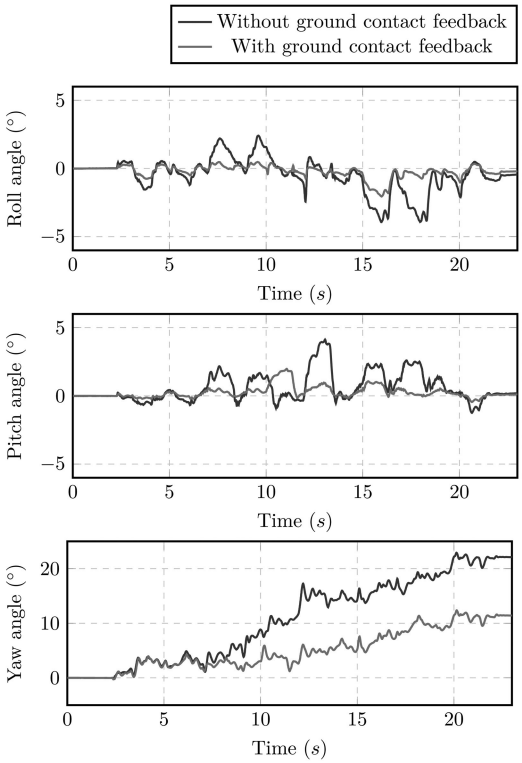

Figure 14. The attitude variations during walking with and without ground contact feedback (without yaw angle correction).

In the second experiment, the yaw angle correction algorithm was disabled, and the experimental results are shown in Fig. 14 and Table 3. The experimental results show that despite some fluctuations in yaw angles, no large drifts were observed as the situation in Fig. 13, even when walking on uneven ground. And there are distinct yaw angle drifts without yaw angle correction as the situation in Fig. 14. This further demonstrates the effectiveness of the yaw angle correction algorithm.

5. Conclusion

This paper presents feedback control strategies for a hexapod walking robot. Initially, the kinematic model and basic control method of the robot were introduced. To achieve closed-loop strategies, an IMU sensor feedback and the tactile sensor feedback were used in addition to the open-loop basic control method. The paper analyses the yaw angle correction algorithm in both straight gait and turning gait situations using actual yaw angle data from an IMU sensor. A PD controller was utilised in the yaw angle correction algorithm to promptly reduce the yaw angle error during motion. Furthermore, the tactile sensors were employed to detect ground contact of the swing legs, enabling the adjustment of the foot-end trajectory to improve walking performance. The results of the experiments demonstrated the effectiveness of the proposed strategies.

The proposed control strategies are simple yet effective. Specifically, the introduced yaw angle correction method is easy to compute and implement. In comparison, the position-posture trajectory tracking method, proposed in [14], achieves closed-loop control of all attitude angles and positions. However, due to the lack of position feedback, the method is challenging to implement when the robot is walking. Another Walking Posture Control method, presents in [12], employs VMC on a hexapod robot, achieving good posture control performance while walking on uneven terrain. However, the robot's yaw angle during walking was not properly controlled. Moreover, the foot force sensors are required to conduct the foot force distribution and apply the VMC method, which is not cost-effective compared with the tactile sensors. Additionally, the foot force controller requires a greater computational effort, which could lead to a lower control frequency and slower posture response.

Our current research is at a relatively initial stage. Only the yaw angle was corrected during walking, it may not matter much when walking on flat ground, but to achieve locomotion on uneven ground, the feedback

and correction of all attitude angles will be necessary. Additionally, since the attitude is solely reliant on the IMU sensor, it may be susceptible to sensor data drift. Therefore, multi-sensor fusion will be considered in future research to achieve better positioning and closed-loop control effects.

Acknowledgement

This work was supported by the Ningbo Municipal Bureau of Science and Technology under grant 2019B10052.

References

[1] B. You, Y. Fan, and D. Liu, Fault-tolerant motion planning for a hexapod robot with single-leg failure using a foot force control method, *International Journal of Advanced Robotic Systems, 19*(5), 2022.

[2] A. Roennau, G. Heppner, M. Nowicki, and R. Dillmann, LAURON V: A versatile six-legged walking robot with advanced maneuverability, *Proc. 2014 IEEE/ASME International Conf. on Advanced Intelligent Mechatronics*, Besacon, 2014, 82–87.

[3] T. Wimböck, M. Görner, and G. Hirzinger, The DLR Crawler: Evaluation of gaits and control of an actively compliant six-legged walking robot, *Industrial Robot: An International Journal, 36*(4), 2009, 344–351.

[4] J.-Y. Kim, B.-H. Jun, and I.-W. Park, Six-legged walking of "Little Crabster" on uneven terrain, *International Journal of Precision Engineering and Manufacturing, 18*(4), 2017, 509–518.

[5] L. Zhang, D. Li, F. Yang, and C. Liu, Development and attitude control of a Hexapod bionic-Robot, *Proc. 2016 IEEE International Conf. on Robotics and Biomimetics (ROBIO)*, Qingdao, 2016, 77–82.

[6] Y. Liu, C. Wang, H. Zhang, and J. Zhao, Research on the posture control method of hexapod robot for rugged terrain, *Applied Sciences, 10*(19), 2020, 6725.

[7] C. Yu, L. Zhou, H. Qian, and Y. Xu, Posture Correction of Quadruped Robot for Adaptive Slope Walking, *Proc. 2018 IEEE International Conf. on Robotics and Biomimetics (ROBIO)*, Kuala Lumpur, 2018, 1220–1225.

[8] J. Faigl, and P. Čížek, Adaptive locomotion control of hexapod walking robot for traversing rough terrains with position feedback only, *Robotics and Autonomous Systems, 116*, 2019, 136–147.

[9] G. Bledt, M.J. Powell, B. Katz, J.D. Carlo, P.M. Wensing, and S. Kim, MIT Cheetah 3: Design and control of a robust, dynamic quadruped robot, *Proc. 2018 IEEE/RSJ International Conf. on Intelligent Robots and Systems (IROS)*, Madrid, 2018, 2245–2252.

[10] M. Pavone, P. Arena, L. Fortuna, M. Frasca, and L. Patané, Climbing obstacle in bio-robots *via* CNN and adaptive attitude control, *International Journal of Circuit Theory and Applications, 34*(1), 2006, 109–125.

[11] C. Ding, L. Zhou, X. Rong, Y. Li, and J. Gu, A lateral impact recovery method for quadruped robot with step height compensation, *International Journal of Robotics and Automation, 35*(3), 2020, 199–208.

[12] M. Tikam, D. Withey, and N.J. Theron, Posture control for a low-cost commercially-available hexapod robot*, *Proc. 2020 IEEE International Conf. on Robotics and Automation (ICRA)*, Paris, 2020, 4498–4504.

[13] Z. Chen, S. Wang, J. Wang, K. Xu, T. Lei, H. Zhang, X. Wang, D. Liu, and J. Si, Control strategy of stable walking for a hexapod wheel-legged robot, *ISA Transactions, 108*, 2021, 367–380.

[14] G. Chen and B. Jin, Position-posture trajectory tracking of a six-legged walking robot, *International Journal of Robotics & Automation, 34*(1), 2019, 24–37.

[15] W.-S. Ji and B.-K. Cho, Development of a walking algorithm on the uneven terrain for a hexapod robot Little Crabster200, *Advances in Mechanical Engineering, 10*(7), 2018.

[16] L. Fućek, Z. Kovačić, and S. Bogdan, Analytically founded yaw control algorithm for walking on uneven terrain applied to a hexapod robot, *International Journal of Advanced Robotic Systems, 16*(3), 2019.

[17] Y. Isvara, S. Rachmatullah, K. Mutijarsa, D.E. Prabakti, and W. Pragitatama, Terrain adaptation gait algorithm in a hexapod walking robot, *Proc. 2014 13th International Conf. on Control Automation Robotics Vision (ICARCV)*, Singapore, 2014, 1735–1739.

[18] C. Ma, F. Yu, and Z. Luo, Simulations and experimental research on a novel soft-terrain hexapod robot, *International Journal of Robotics and Automation, 30*(3), 2015, 247–255.

[19] R. Altendorfer, N. Moore, H. Komsuoglu, M. Buehler, H.B. Brown, D. McMordie, U. Saranli, R. Full, and D.E. Koditschek, RHex: A biologically inspired hexapod runner, *Autonomous Robots, 11*(3), 2001, 207–213.

[20] H. Deng, G. Xin, G. Zhong, and M. Mistry, Gait and trajectory rolling planning and control of hexapod robots for disaster rescue applications, *Robotics and Autonomous Systems, 95*, 2017, 13–24.

[21] H. Yu, H. Gao, L. Ding, M. Li, Z. Deng, and G. Liu, Gait generation with smooth transition using CPG-based locomotion control for hexapod walking robot, *IEEE Transactions on Industrial Electronics, 63*(9), 2016, 5488–5500.

[22] L. Chen, G. Zhong, Y. Hou, W. Zhuo, and W. Nie, The control of a multi-legged robot based on Hopf oscillator, *Proc. 2017 IEEE 3rd Information Technology and Mechatronics Engineering Conf. (ITOEC)*, Chongqing, 2017, 371–375.

[23] W. Zhang, Q. Gong, H. Yang, and Y. Tang, CPG modulates the omnidirectional motion of a hexapod robot in unstructured terrain, *Journal of Bionic Engineering*, *20*, 2023, 558–567.

[24] Y. Zhu and B. Jin, Compliance control of a legged robot based on improved adaptive control: Method and experiments, *International Journal of Robotics and Automation, 31*(5), 2016, 366–373.

[25] Z. Hua, X. Rong, Y. Sun, Y. Li, H. Chai, and C. Wang, A Novel Passive Compliance Method for Hydraulic Servo Actuator Applied on Quadruped Robots, *International Journal of Robotics and Automation, 37*(1), 2022, 76–87.

[26] F. Zhang, S. Zhang, Q. Wang, Y. Yang, and B. Jin, Straight gait research of a small electric hexapod robot, *Applied Sciences, 11*(8), 2021, 3714.

Biographies

Qian Wang was born in Shanxi, China, in 1998. He received the B.S. degree in mechatronic engineering from Zhejiang University, Hangzhou, China, in 2019, where he is currently pursuing the Ph.D. degree in mechatronic engineering. His research interests include robotics, legged robot, and robotic design and control application.

Bo Jin was born in Jiangsu, China, in 1971. He received the B.S. and Ph.D. degrees in fluid power transmission and control from Zhejiang University, Hangzhou, China, in 1993 and 1998, respectively, where he is currently a Professor with the School of Mechanical Engineering. His areas of research include robotic design and control application, hydraulic-legged robot, and electrohydraulic control system.

Ce Zhang was born in Henan, China, in 1981. He received the B.S. degree in mechatronic engineering from Zhejiang University, Hangzhou, China, in 2005. He is currently a Senior Engineer with Ningbo Hoyea Machinery Manufacture Co., Ltd. He is engaged in the research and development of components and systems in electrohydraulic products.

Shidong Zhang was born in Heilongjiang, China, in 1996. He received the B.S. and master's degrees in mechatronic engineering from Zhejiang University, Hangzhou, Zhejiang, in 2018 and 2021, respectively. His areas of research include legged robot design, robotics, and automation control.